

# Large $p_T$ Forward Transverse Single Spin Asymmetries of $\pi^0$ Mesons at $\sqrt{s} = 200$ and 500 GeV from STAR.

---

Steven Heppelmann\* (Penn State University for the STAR Collaboration)

*E-mail:* [heppel@psu.edu](mailto:heppel@psu.edu)

The STAR collaboration has collected two large data sets for measurement of forward  $\pi^0$  transverse single spin asymmetries (SSA) in polarized pp collisions. Preliminary results are presented for data from two RHIC runs, from Run 11 (2011) with energy  $\sqrt{s}=500$  GeV and with luminosity of  $22 \text{ pb}^{-1}$  and from Run 12 (2012) with  $\sqrt{s}=200$  GeV and with luminosity of  $18 \text{ pb}^{-1}$ . Neutral pions are measured with the STAR forward electromagnetic calorimeter with nearly full azimuthal acceptance over the range of pseudo-rapidity from 2.65 to 4.0. Large transverse SSA is now seen over a much greater range of transverse momentum, up to 10 GeV/c, than reported in previous publications. The analysis of the underlying event structure raises important questions about the overall jet-like nature of events associated with the spin asymmetry of the  $\pi^0$ . These results may provide new insight into the 30 year old puzzle as to the nature of large SSAs in forward hadron production.

*XXI International Workshop on Deep-Inelastic Scattering and Related Subjects  
22-26 April, 2013  
Marseilles, France*

---

\*Speaker.

## 1. Introduction

The FMS, an electromagnetic calorimeter, is part of the STAR detector at RHIC. It is located about 7 meters from the interaction region and it detects forward electromagnetic particles relative to the direction of the RHIC blue beam. As seen in Figures 1 and 2, the FMS is an array of lead glass cells where shower photons are detected by photo-multiplier tubes. It contains a central square array of smaller cells (3.8x3.8 cm) embedded in an array of larger cells (5.8x5.8 cm). The detector has nearly full azimuthal acceptance from pseudo-rapidity  $2.6 < \eta < 4.0$ . Data are presented from two recent STAR runs with transversely polarized pp collisions. Run 11 (2011) involved pp collisions at  $\sqrt{s} = 500$  GeV and Run 12 (2012) with  $\sqrt{s} = 200$  GeV. These two data sets are characterized by 22 and 18  $pb^{-1}$  of integrated luminosity and average blue beam transverse polarizations of 51.6% and 60.7% respectively. We will present the preliminary measurements of the  $\pi^0$  single spin asymmetry  $A_N$  over a wider range of transverse momentum than has been reported by STAR previously [1].

The transverse asymmetry is defined by the ratio of difference to sum of spin up and spin down cross section when the forward  $\pi^0$  emerge to the left,  $A_N = \frac{\sigma_L^\uparrow - \sigma_L^\downarrow}{\sigma_L^\uparrow + \sigma_L^\downarrow}$ . This analysis will investigate the dependence of the forward  $\pi^0$  transverse asymmetry on the topology of the background event. In particular, we will find that  $A_N$  is sensitive to the details of the degree of isolation in the vicinity of the produced  $\pi^0$ . It is expected in conventional PQCD related models, based on the Collins effect [2], that the production of higher energy and transverse momentum pions involves hard parton scattering and fragmentation of a jet.  $A_N$  is non-zero because of an asymmetry of the fragmentation process. A broad class of PQCD based models require  $A_N$  to fall with  $p_T$  and that the  $\pi^0$  be accompanied by additional fragmentation hadrons, some of which will deposit electro-magnetic energy in the FMS.

## 2. Data Selection

In the FMS analysis, photon candidates consist of localized energy in one or more adjacent lead glass cells with energy distributed in accordance with expectation for electromagnetic showers. The data are processed in a first pass where these photon candidates with localized energy greater than a noise cutoff  $E_{soft} = 0.75$  GeV in the large cells region or 2.0 GeV in the small cell region are identified.

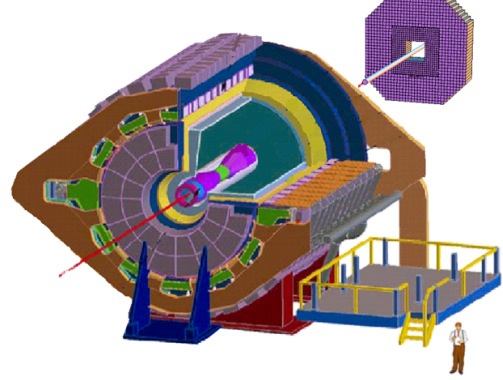


**Figure 1:** The STAR Detector at RHIC in foreground and FMS in the rear.

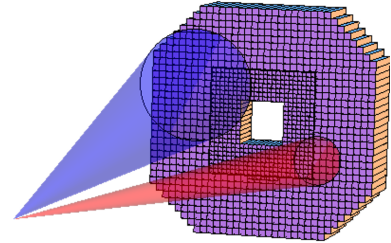


**Figure 2:** The FMS electromagnetic calorimeter. Examples of two cones with half angle sizes of 35 mR (red) and 70mR (blue) are shown.

Next, a more selected photon list is created to contain the photon candidates with energy  $E > E_{min}$ , with  $E_{min}=6$  GeV (4 GeV for large cells Run 11). The list of photons is sorted with an algorithm, similar to a jet reconstruction algorithm, with photon candidates added to a cluster of photons when they are produced at an angle relative to the center of the cluster that is less than a fixed cone radius. The number of such photons within the chosen angular cone is  $N_\gamma$ . The number of remaining photon candidates with energies  $E_{soft} < E < E_{min}$  is  $N_{soft}$ . The Run 11 500 GeV data were analyzed with both 30mR and 70mR cone radii. The Run 12 200 GeV data were analyzed with 35mR, 70mR and 200mR cone sizes. The 200mR cone covers most of the FMS detector and the 35mR and 70mR cones are shown relative to the detector size in Figure 2.

For events that satisfy a FMS hardware trigger based on a hardwired localized transverse energy sum,  $\pi^0$  events are identified with the following selection cuts.

1. Exactly two photons ( $N_\gamma = 2$ ) of energies  $E_1 > E_{min}$  and  $E_2 > E_{min}$ .
2. Selection of a di-photon Mass  $M_{1,2}$  range ( $M_{1,2} < 0.4 GeV/c^2$  for 200 GeV data).
3.  $Z \equiv \left| \frac{E_1 - E_2}{E_1 + E_2} \right| < 0.7$ .

The above criteria are applied with specification of an analysis cone angle 30mR, 35mR, 70mR or 200 mR and sorted by the number of soft photons candidates,  $N_{soft}$ . All asymmetries shown are plotted with statistical error bars and the preliminary fractional systematic errors are  $\frac{\delta A_N}{A_N} < 15\%$ .

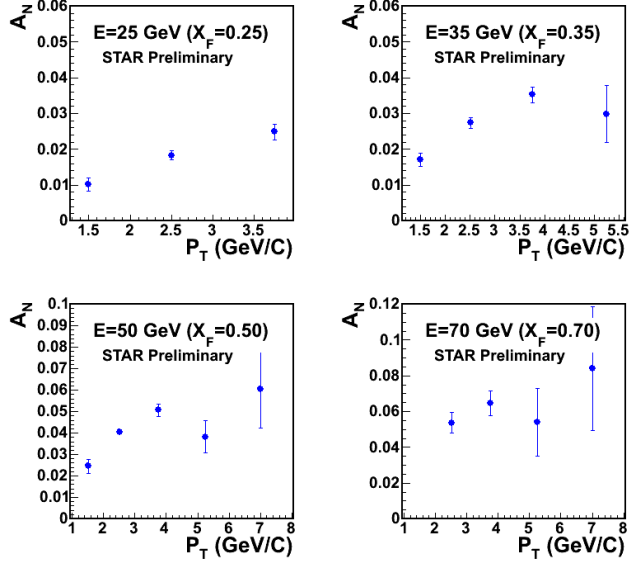


**Figure 3:** Transverse Single Spin Asymmetry  $A_N$  measured at  $\sqrt{s} = 200$  GeV in the FMS using a 35 mR cone algorithm to identify  $\pi^0$  events.  $A_N$  is plotted vs.  $\pi^0$  transverse momentum.

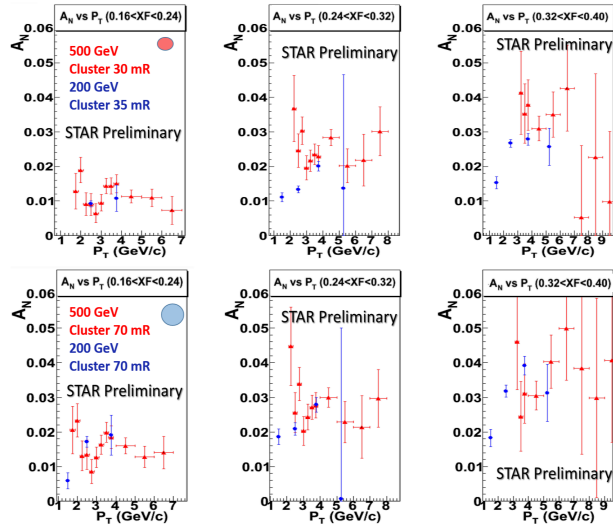


**Figure 4:** A comparison between the 500 GeV (red) and 200 GeV (blue) transverse single spin asymmetry  $A_N$  for production in the range of Feynman  $X_F < 0.4$ . The upper plots show the results with smaller cone sizes used for event selection. No  $N_{soft}$  cut has been applied for these plots.

### 3. Run 11: 200 GeV

In Figure 3 we show the distribution of  $A_N$  for  $\pi^0$  selected from the Run 12 data set. The event set was created with a cone size of 35 mR and with  $N_{soft} = 0$ . We observe a clear increase in the asymmetry with transverse momentum up to transverse momentum in the 5 to 7 GeV/c range. The mass cut for this data set is  $0 < M_{1,2} < 0.4 GeV$ , leading to non  $\pi^0$  background less than 10%. Data are shown in four Feynman  $X_F$  ranges.

### 4. Run 12: 500 GeV

At 500 GeV, the  $\pi_0$  identification in the FMS extends through Feynman  $X_F < 0.4$ . In Figure 4, the same 200 GeV data have been binned in Feynman  $X_F$  for comparison with Run 11 500 GeV data. Analysis is performed at each energy for two cone sizes. The cuts for the 500 GeV data points are  $0.015 < M_{1,2} < 0.255 GeV$ . The cone selection sizes are 30 mR and 70 mR at 500 GeV and the cone sizes are 35 mR and 70 mR at 200 GeV. In the same  $X_F$  range, the 500 GeV data extends to larger transverse momentum  $p_T$  than the 200 GeV measurement. In the lower  $p_T$  region where the coverage overlaps, the asymmetry may grow slowly with energy but the scale of  $A_N$  is similar at the two energies. For both energies, we see a general trend that the larger cone size, indicating more isolated  $\pi^0$  topology, leads to a larger value of single spin asymmetry.

### 5. Dependence on Isolation

We look further at the dependence of  $A_N$  on the degree of isolation of the  $\pi^0$  with data from the 200 GeV data set. In Figure 5 we show plots of  $A_N$  vs. pseudo-rapidity but plotted for different choices of cone size and  $N_{soft}$ . In Figure 5 we show  $A_N$  for three choices of cone size and requirements on the soft photon background. The data are presented with 3 variations in analysis:

1. 200 mR cone and  $N_{soft} = 0$
2. 70 mR cone and  $N_{soft} = 0$
3. 35 mR cone and  $N_{soft} > 0$

These three selection criterion correspond to a progression from the selection of the most isolated  $\pi^0$ 's to selection of events with observed jet-like fragments. In particular in the low pseudo-rapidity regions (largest  $p_T$ ) and at lower  $X_F$ , the asymmetry is much smaller when evidence for nearby fragments is observed.

Another approach that addresses a similar question of topology involves the distribution of secondary (35 mRad) cones of photon(s) within the event containing a primary  $\pi^0$ . The idea is

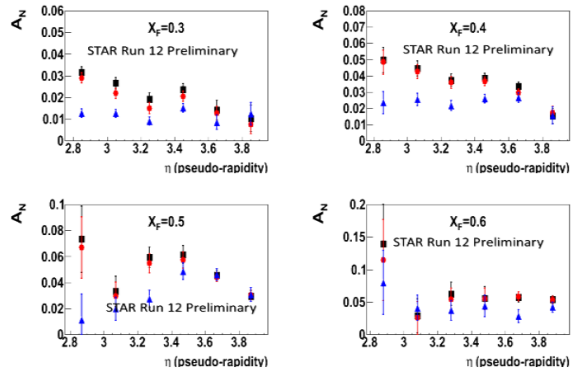


**Figure 5:**  $A_N$  vs. pseudo-rapidity  $\eta$  for different  $\pi^0$  selection criterion. For plotted data, two photons are found in the cone and fall in the  $\pi^0$  mass region. Black squares: 200mR cone and no soft photons. Red circles: 70 mR cone and no soft photons. Blue triangles: 35 mR cone and soft photons observed.

to investigate the dependence of  $A_N$  for primary  $\pi^0$  production if there are additional photons outside the primary  $\pi^0$  cone, at an energy weighted average azimuthal angle  $\phi$  relative to the original  $\pi^0$  direction. The analysis shown in Figure 6 represents a study of three classes of event selection involving a possible second cone of photons at azimuthal angle  $\phi$  from the principle  $\pi^0$ . Three selections define the three sets shown in Figure 6.

1. 1 cone events
2. 2 cones  $\cos(\phi) < -0.5$
3. 2 cones  $\cos(\phi) > 0$

The conclusion is that the asymmetry is reduced if there is a second photon cone in the same hemisphere as the principle  $\pi^0$  from which asymmetry is derived.

We note that the difference in  $A_N$  between events with same side fragments and away side fragments is greater in the lower  $X_F$  ( $X_F < 0.45$ ) region. It was further observed that if the second cone contains a two photon  $\pi^0$ , the trend is similar, with small asymmetry if the lower energy  $\pi^0$  is on the same hemisphere as the primary  $\pi^0$  but larger asymmetry when the  $\pi^0$  is in the opposite hemisphere.

For decades it has been known that transverse single spin asymmetries are suppressed in conventional collinear factorized PQCD. It is always exciting to speculate that the predominance of forward  $A_N$  is an indication of new order in scattering beyond conventional PQCD. Models have been developed to push collinear PQCD to extend its application and reach beyond current limits. Among these models are those based on Collins fragmentation [2] where the asymmetry suppressed in the hard process emerges only from the asymmetric fragmentation of a jet. Consistent with the higher twist PQCD, current models predict a falling off of  $A_N$  with transverse momentum.

To summarize, the measurements of  $A_N$  for forward  $\pi^0$  production has been extended to higher  $p_T$  at  $\sqrt{s} = 200$  and 500 GeV with no observed falloff at larger  $p_T$ . For events that show evidence of jet fragmentation, the forward  $\pi^0$  single spin asymmetry is much reduced when compared to events where the  $\pi^0$  emerges with greater isolation. This may raise interesting questions about the role of fragmentation in this historically mysterious phenomena of the large forward asymmetries and perhaps the role and nature of factorized PQCD [3] for events that produce these asymmetries.

## References

- [1] B. I. Abelev *et al.* [STAR Collaboration], Phys. Rev. Lett. **101**, 222001 (2008) [arXiv:0801.2990 [hep-ex]].
- [2] J. C. Collins, S. F. Heppelmann and G. A. Ladinsky, Nucl. Phys. B **420**, 565 (1994) [hep-ph/9305309].
- [3] T. C. Rogers, arXiv:1304.4251 [hep-ph].

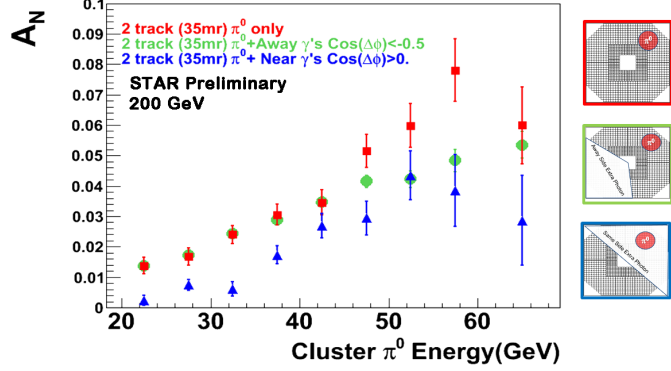


**Figure 6:** The two photon Energy ( $E_{1,2}$ ) dependence of the transverse single spin asymmetry at  $\sqrt{s}=200$  GeV. Note that  $X_F = \frac{E_{1,2}}{100\text{GeV}}$ . The three colors correspond to the observation and location of additional photon energy as enumerated in the text. 1) Red squares; 2) Green circles; 3) Blue triangles.